IEEE Access
Multidisciplinary | Rapid Review | Open Access Journal

Received October 26, 2021, accepted November 15, 2021, date of publication November 17, 2021,
date of current version November 29, 2021.

Digital Object Identifier 10.1109/ACCESS.2021.3128967

A Resilience Assessment Framework for Distribution Systems Under Typhoon Disasters

YUANTAO WANG[1], TIANEN HUANG[1], XIANG LI[1], JIAN TANG[1], ZHENJIE WU[1], YAJUN MO[1], LIN XUE[2], YIXI ZHOU[1], TAO NIU[2], (Member, IEEE), AND SICONG SUN[1]

[1]State Grid Hangzhou Power Supply Company, Hangzhou 310020, China
[2]State Key Laboratory of Power Transmission Equipment and System Security and New Technology, Chongqing University, Chongqing 400044, China

Corresponding author: Tao Niu (niutthu@qq.com)

This research was funded by Science and technology projects of State Grid Zhejiang Electric Power Co., Ltd. 2021ZK37 (Research on partition coordinated self-healing recovery technology of power system based on artificial intelligence).

ABSTRACT With the increase of extreme natural disasters and the frequent occurrence of man-made attacks, resilience studies of power grids have attracted much attention, among which resilience assessment reflects the resistance and resilience of power systems to cope with extreme disasters. To improve the resilience of distribution grids under extreme weather conditions, this paper proposes a resilience assessment framework for distribution grids under typhoon disasters. First, a probabilistic generation model of typhoon is established. Second, a spatiotemporal vulnerability model of the distribution grid lines to quantify the spatiotemporal impacts of typhoon. Third, a breadth-first search algorithm is used to island the distribution grid, and the amount of load shedding of the islanded microgrid is calculated. Meanwhile, the resilience of the distribution grid was quantitatively assessed according to the proposed new resilience index. Finally, the feasibility of the proposed resilience assessment method is verified in the IEEE 33-bus test system, and the results show that the proposed method can accurately account for the impact of typhoon on the distribution grid and provides a quantitative reference basis for later power system planning and scheduling.

INDEX TERMS Vulnerability model, resilience assessment, island division, resilience index.

I. INTRODUCTION

The impact of extreme weather on power grids has received widespread attention, such as the snowstorm in China in 2008 and Hurricane Sandy in the United States in 2012, which cause to grid lines damage and tower toppling, widespread power outages and huge economic losses [1]. In extreme weather conditions, multiple failures often occur in the distribution grid, and the N-1 safety criterion of the distribution grid alone is not sufficient to guarantee the safe operation of the distribution grid. Resilience is defined as the ability of the grid to withstand and recover from small probability of extreme events [2]. Besides, as the distribution grid has the closest relationship with the user's production and life, the resilience of the distribution grid is mainly manifested by the support and recovery ability of the critical load in the distribution grid under extreme weather events. The resilience assessment of the distribution grid is of great significance for the safe operation and planning of the distribution grid.

The associate editor coordinating the review of this manuscript and approving it for publication was Jason Gu.

Typhoons, one of the most common extreme disasters, have an impact on the failure rate of the lines of the power grid, which in turn may cause to system load shedding and economic losses. This study focused on the impact of typhoons on distribution grids. Therefore, it is necessary to establish the model of the wind fields of typhoons. Several studies have also studied the model of typhoons. The Ref. [3] proposed a stochastic method to simulate typhoon trajectories based on historical data, which is seriously dependent on historical data. Thereafter, the Batts wind field model was proposed in [4], which is a more mature wind field model. [5] proposed the Georgiou typhoon wind field model, which can more accurately forecast the wind speed of typhoon when the typhoon is moving on the sea surface. [6] proposed a method for simulating a typhoon wind field based on SPARK for high-performance computing. The [7] captured the overall variability of the typhoon based on a hierarchical network and accurately accounted for the wind speed at the geographical location of typhoon. However, this modeling for typhoons does not consider the probability of typhoon occurrence, which is necessary to consider the probability of typhoon

scenario generation in the long-term planning and construction of power systems.

To construct a model for the impact of typhoons on distribution grids, [8] proposed a formula for calculating the magnitude of wind speed within a wind field and used a fragility curve to calculate the reliability of distribution grid lines. The [9] used typhoon historical data to determine the typhoon center shift speed and used the lognormal cumulative distribution function to evaluate the reliability of overhead conductors and poles. The [10] established a line failure rate model based on the spatial and temporal characteristics of typhoon damage to distribution grid lines. The [11]–[13] constructed the vulnerability curves in a wind speed environment based on the location of the component in the wind field of typhoon. However, the actual distribution system is generally widely distributed in a radial pattern in space, and when a typhoon passes through the distribution grid, the wind speeds are different in different line segments of the distribution grid. Therefore, it is necessary to establish an accurate spatiotemporal vulnerability model for the impact of typhoons on the distribution grid.

In terms of resilience assessment, some computational indexes for resilience assessment are proposed in previous studies. References [14]–[16] proposed a quantitative criteria, which is obtained by calculating dimensionless metrics a distribution system. The [17] proposed a new resilience index considering the duration of extreme events. The [18] proposed six indicators to qualitatively evaluate the architecture of smart grid in a disturbed environment. The [19] proposed a set of metrics to quantify the resilience of the system to the impact of disruptions from extreme events. However, while these resilience indexes can reflect the degree of system recovery during disasters, the resilience indexes also have to capture the inherent uncertainty associated with the resulting degradation of system performance.

As seen above, when studying the impact of typhoon disasters on distribution systems, the spatial and temporal characteristics of typhoon disasters are not fully considered in some of the studies, and the process of component failure rates changing over time is ignored. The intensity and location of actual typhoons constantly change with time, and the typhoon has different impacts on components in different locations. At the same time, some of the resilience indexes are calculated based on the state operation curve of the system, without considering the uncertainty of typhoon disasters, which causes to the limitations of the indexes in practical applications. Therefore, this paper establishes a resilience assessment framework for distribution systems under typhoon disasters. The resilience of the distribution system can be comprehensively assessed by analyzing the impact of various potential typhoon hazards on the distribution grid lines. The weak points of the system can be accurately identified, and a reference basis for distribution grid planning can be provided. The main contributions of this paper are as follows.

1) By establishing the distribution functions of each key parameter of the typhoon, the spatial and temporal probability model of the typhoon is established to lay the foundation for the subsequent establishment of the vulnerability model of distribution grid lines.

2) To quantify the impact of typhoons on lines, a vulnerability model of distribution grid lines is established and the cumulative failure probability density function of each line is constructed to lay the foundation for the subsequent resilience assessment model.

3) Considering the vulnerability of lines under typhoon disasters, the breadth-first search algorithm is used to island the distribution grid. Meanwhile, the optimal load shedding of each islanded microgrid is calculated separately. Then, the new resilience index is defined that calculate the sum of the product of the probability of typhoon occurrence and the optimal load shedding in each island microgrid, which is used to quantify the impact of typhoons on the distribution system.

The detailed research framework of this paper is shown in Figure 1. This paper is organized as follows. The typhoon probabilistic model is described in Section II. The vulnerability model of the lines and poles of the distribution grid units is established in Section III. Section IV is the whole resilence assessment model, where the breadth-first search algorithm is used to island the distribution grid based on the vulnerability model of distribution grid lines under a typhoon scenario and the new resilence index is caluculated in each islanded microgrid. In Section V, the feasibility of the proposed resilience assessment method is verified in the IEEE 33-bus test system. Section VI summarizes the whole research.

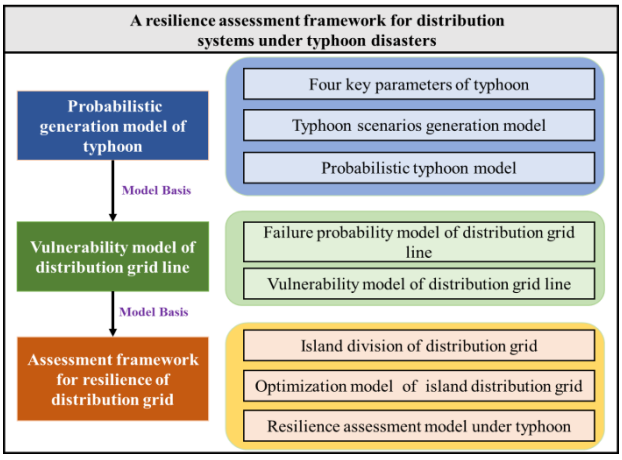

FIGURE 1. The research framework of this paper.

II. TYPHOON WIND FIELD MODELING

A. TYPHOON MODEL

Typhoon is a tropical cyclone. A tropical cyclone is a low-pressure vortex that occurs in tropical or subtropical oceans. After a typhoon is formed, it generally moves out from its source and go through an evolutionary process

of development, maturation, weakening, and extinction. A developed and mature typhoon typically has a cyclonic radius of 500 km - 1000 km and an altitude of up to 15 km - 20 km. Typhoons consist of three parts: the peripheral area of Typhoon, maximum wind speed, and typhoon eye [20]. The impacts of typhoons can also be broadly classified into three categories: 1) typhoons continue to move deeper into the land after lading via the coastline and affect the surrounding structures; 2) typhoons form cyclones on sea and affect the land through the surrounding clouds; and 3) typhoons move back and forth after landing and affect the land. This paper focuses on the impact of typhoon intensity and duration on distribution lines after landing. To accurately assess the impact of the typhoon model on distribution grid lines, this section establishes a detailed typhoon model based on the location of typhoon landing, central pressure difference, wind speed, maximum radius, and typhoon movement speed.

Among them, the typhoon central pressure difference, defined as the difference between the typhoon peripheral pressure and the typhoon central pressure. The peripheral pressure is usually one standard atmosphere is taken as 1013 hpa to characterizes the initial intensity of the typhoon, which determines the maximum wind speed within the wind field after the typhoon landing. The decay model of the typhoon pressure difference at a moment t when the typhoon passes over land is expressed as:

$$\Delta P(t) = \Delta P(0) - 0.02 \times [1 + \sin(\alpha - \beta)] \times t \tag{1}$$

where α denotes the angle between the coastline where the typhoon landing and due north; β denotes the angle between the direction of typhoon motion and due north, and t denotes the time of typhoon motion. $\Delta P(0)$ is the pressure difference between the typhoon center at the moment of typhoon landing.

The wind speed at the maximum radius of a typhoon can be characterized as:

$$\begin{aligned} v_{r\max}(t) &= 0.865 \times v_{gt}(t) + 0.5 \times v_T \\ &= 0.865 \times \lambda \times \sqrt{\Delta P(t)} + 0.5 \times v_T \end{aligned} \tag{2}$$

where v_T is the speed of motion of the typhoon, v_{gt} is the gradient wind speed, which is generated by the airflow due to the pressure gradient. λ is a constant, typically taking a value of 6.97.

The wind speed at any point in a typhoon wind field can be expressed by the following equation.

$$v_r(t) = \begin{cases} v_{r\max}(t) \times [d(t)/r_{\max}(t)] & when\ d(t) \le r_{\max} \\ v_{r\max}(t) \times [r_{\max}(t)/d(t)]^{\eta} & when\ d(t) > r_{\max} \end{cases} \tag{3}$$

where $v_{r\max}$ is the wind speed at the maximum radius in the wind field of typhoon, d is the distance from a point in the actual geographic location to the center of the wind field, and $r_{\max}$ is the maximum radius of the wind field of typhoon. η is usually taken as [0.5,0.7], and 0.6 in this paper.

Figure 2 shows a schematic diagram of the impact of a typhoon on a distribution grid lines. The maximum radius of

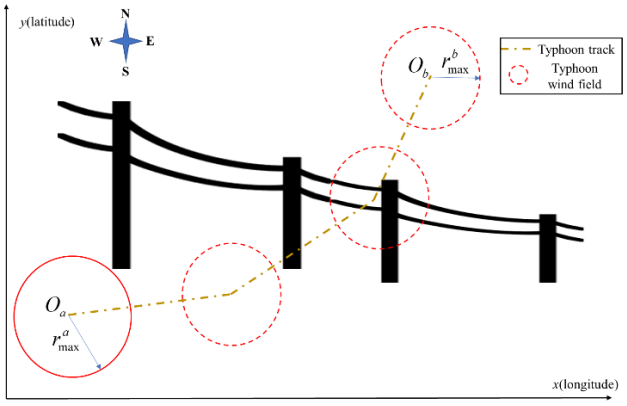

FIGURE 2. Diagram of the impact of typhoons on distribution grid lines.

a typhoon can be expressed using the following equation.

$$v_{\max} = \exp[-0.1239 \times \Delta P(t)^{0.6} + 5.1034] \tag{4}$$

B. TYPHOON SCENARIO GENERATION MODEL

According to the typhoon model established in the previous section, to generate a typical typhoon scenario to study the impact on the distribution grid, four parameters are first selected to generate a typhoon scenario: the location of the typhoon landing, the pressure difference at the center of the typhoon, the direction of typhoon motion, and the speed of typhoon movement. A typhoon generation scenario can be determined based on these four core parameters.

Assuming that the pressure difference between the original centers obeys a log-normal probability distribution, the probability distribution function of the central pressure difference of the typhoon as shown in (5).

$$f(\Delta P) = \frac{1}{0.6274 \Delta P \sqrt{2\pi}} \exp\left(-\frac{(\ln \Delta P - 2.9001)^2}{2 \times 0.6274^2}\right) \tag{5}$$

Assuming that the movement speed of the typhoon obeys the log-normal probability distribution, the probability distribution function of the movement speed of the typhoon as shown in (6).

$$f(v_T) = \frac{1}{0.5185 v_T \sqrt{2\pi}} \exp\left(-\frac{(\ln v_T - 2.6680)^2}{2 \times 0.5185^2}\right) \tag{6}$$

Assuming that the direction of motion obeys a paranormal probability distribution, the probability distribution function of the direction of motion as shown in (7).

$$\begin{aligned} f(\alpha) = &\frac{0.5035}{22.5891\sqrt{2\pi}} \exp\left[-\frac{(\alpha + 73.3392)^2}{2 \times 22.5891^2}\right] \\ &+ \frac{1 - 0.5035}{70.3532\sqrt{2\pi}} \exp\left[-\frac{(\alpha + 7.2084)^2}{2 \times 70.3532^2}\right] \end{aligned} \tag{7}$$

Assuming that the location of typhoon landing obeys uniform probability distribution, the probability distribution function of the location of typhoon landing as shown in (8).

$$f(x_0) = \frac{1}{b_x - a_x}, \quad f(y_0) = \frac{1}{b_y - a_y} \tag{8}$$

where (a_x, a_y) and (b_x, b_y) are the coordinates of the starting and ending points of the shoreline in the study area, respectively.

The occurrence probability of each parameter of a typhoon is calculated as shown in (9), taking the central pressure difference of the typhoon as an example: First, the probability density function of the central pressure difference is divided into N equal parts with step size h. According to the probability density function, the occurrence probability of the central pressure difference of a typhoon can be calculated as follows.

$$\Pr(\Delta P) = \int_{\Delta P - h/2}^{\Delta P + h/2} f(\Delta P) d\,\Delta P \tag{9}$$

The probability of the other core parameters is calculated as shown above, and the occurrence probability model of a typhoon is as follows.

$$\boldsymbol{Pr_t} = \{Pr(\Delta P), Pr(v_T), Pr(\alpha), Pr(x, y)\}_K \tag{10}$$

$$Pr_w = \left\| \bigotimes_{i=1}^{K} \boldsymbol{Pr_t} \right\| = \prod_{i=1}^{K} \|\boldsymbol{Pr_t}\| \tag{11}$$

The numerical magnitudes of the four key parameters of the typhoon and the corresponding typhoon probabilities are selected by random sampling. The random sampling algorithm flow as follows.

TABLE 1. Random sampling algorithm flow.

STEP1	Select the initial operation points $\Delta P(0)$, $v_T(0)$, $\alpha(0)$ and (x_0, y_0) of the four parameters.
STEP2	Determine the interval of the four parameters of the typhoon, $\left[\Delta P(0)-\Delta P, \Delta P(0)+\Delta P\right]$, $\left[v_T(0)-\Delta v_T, v_T(0)+\Delta v_T\right]$, $\left[\alpha(0)-\Delta\alpha, \alpha(0)+\Delta\alpha\right]$, $[(x,y) \mid x \in (x_0-\Delta x, x_0+\Delta x), y \in (y_0-\Delta y, y_0+\Delta y)]$.
STEP3	Generate several random number vectors uniformly distributed in the four parameter intervals, $\boldsymbol{\Phi}=[\Phi_{\Delta P}\ \Phi_{v_T}\ \Phi_{\alpha}\ \Phi_{x,y}]$. Set the initial iteration value to $i = 1$.
STEP4	The random number vector $\boldsymbol{\Phi}$ are randomly arranged, and the first element from each vector element is taken to form the basis parameter, $\boldsymbol{X} = \left[\Delta P^i\ \ v_T^{\,i}\ \ \alpha^i\ \ (x,y)^i\right]$.
STEP5	Calculate the probability $\boldsymbol{F} = \left[f^i(\Delta P)\ \ f^i(v_T)\ \ f^i(\alpha)\ \ f^i(x,y)\right]$ corresponding to $\boldsymbol{X}$.
STEP6	Calculate the probability of typhoon generation scenario according to (11).
STEP7	Set the number of selected scenarios to N, and output the parameters of the typhoon scenarios $\boldsymbol{X}$, $\boldsymbol{F}$, Pr_w.

III. THE VULNERABILITY MODEL OF DISTRIBUTION GRID LINES UNDER TYPHOON

A. FAILURE RATE MODEL FOR DISTRIBUTION GRID LINES

The two main factors of typhoon impact on the distribution grid are typhoon wind speed and typhoon duration. When a typhoon occurs, if the distribution grid is experiencing by the typhoon, the lines and poles of the distribution grid are highly vulnerable to damage and failure, which will result in forced load shedding operation of the whole system. Therefore, this section establishes the relationship between the typhoon wind speed and the failure rate of lines and poles in the distribution grid.

The equation of the failure rate of the distribution grid poles is as follows.

$$\lambda_{pl,i}(t) = \begin{cases} 0, & v_{pl,i}(t) \in [0, v^*_{pl}] \\ \exp[0.2(v_{pl,i}(t) - 2v^*_{pl})], & v_{pl,i}(t) \in [v^*_{pl}, 2v^*_{pl}] \\ 1, & v_{pl,i}(t) \in [2v^*_{pl}, \infty] \end{cases} \tag{12}$$

where the failure rate of the pole is modeled as a segmental function, v^*_{pl} denotes the maximum wind speed that the pole can withstand, 35 m/s is taken, and $v_{pl,i}(t)$ denotes the typhoon wind speed that the i-th pole can withstand at moment t.

The failure rate model of the lines of the distribution grid is as follows.

$$\lambda_{line,j}(t) = \exp[11 \times \frac{v_{line,j}(t)}{v^*_{line}} - 18] \tag{13}$$

where v^*_{line} is the maximum wind speed that the distribution grid lines can withstand, take 20 m/s here, $v_{line,j}(t)$ indicates the typhoon wind speed at the end of the j-th line.

B. THE VULNERABILITY MODEL OF DISTRIBUTION GRID LINES

Based on the failure rates of distribution grid lines and poles in the previous section, we obtain the cumulative failure probability density function for poles and lines, respectively.

$$\begin{aligned} FP_{pl,i} &= 1 - \exp\{-\int_0^T [\lambda_{pl,i}/(1-\lambda_{pl,i})]\}dt \\ &= 1 - \exp\{-\sum_{i=0}^{N-1}\int_0^T [\lambda_{pl,i}/(1-\lambda_{pl,i})]dt\} \\ &= 1 - \exp\{-\sum_{i=0}^{N-1} [\lambda_{pl,i}/(1-\lambda_{pl,i})]\Delta t\} \end{aligned} \tag{14}$$

$$\begin{aligned} FP_{line,j} &= 1 - \exp(-\int_0^T \lambda_{line,j}dt) \\ &= 1 - \exp[-\sum_{i=0}^{N-1}\int_t^{t+\Delta t} \lambda_{line,j}(t)dt] \\ &= 1 - \exp[-\sum_{i=0}^{N-1} \lambda_{line,j}(t)\Delta t] \end{aligned} \tag{15}$$

The failure probability of the entire distribution system is obtained from the series-system reliability equation as follow in (16).

$$FP_{i,j} = 1 - \prod_{1}^{I}(1-FP_{pl,i})\prod_{1}^{J}(1-FP_{line,j}) \tag{16}$$

where I is the total number of poles, and J is the total number of distribution grid lines. The distribution grid lines and poles are in series, so the failure probability of the entire distribution system is $FP_{i,j}$.

IV. A RESILIENCE ASSESSMENT FRAMEWORK FOR DISTRIBUTION SYSTEMS UNDER TYPHOON DISASTERS

A. BREADTH FIRST SEARCH ALGORITHM

The distribution grid is usually radial. Assuming that a distribution grid has n nodes and b branches, the distribution grid can be regarded as a directed incidence matrix A.

For example:

$$A = \begin{bmatrix} 1 & 0 & 0 & 0 \\ -1 & 1 & 0 & 1 \\ 0 & -1 & 1 & 0 \\ 0 & 0 & -1 & 0 \\ 0 & 0 & 0 & -1 \end{bmatrix}_{n\times b} \tag{17}$$

Among them, 1 indicates the start node and -1 indicates the end node. If a branch is damaged by a typhoon, both the start and end node are set to 0. To quickly partition a node association matrix, this section adopts the breadth first search (BFS) algorithm to traverse the distribution grid line status after the typhoon landing, and place the faulty line in the set **B**. The corresponding first and last nodes are counted as 0, and then BFS is used to calculate the result of the distribution grid splitting and zoning caused by the typhoon. The specific process is as follows.

According to the above process, the matrix block diagram of matrix A is drawn as shown in Figure 3:

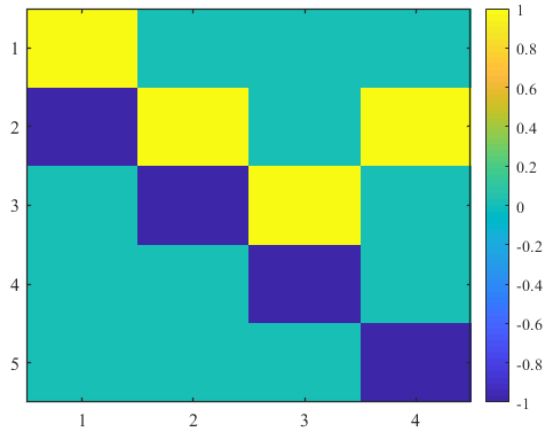

FIGURE 3. The matrix block diagram of *A*.

Assuming that the typhoon caused the failure of the line between the first node 2 and the last node 3, the matrix A^* under the typhoon disaster is constructed, then the search path of each partition is obtained by the BFS algorithm as shown in Figure 4, and it is also divided into two zones accordingly.

TABLE 2. Breadth first search algorithm.

STEP1	Initialize the directed incidence matrix and construct a matrix graph. Yellow represents the start node and blue represents the end node.
STEP2	According to the random sampling results, the first node and the last node of the faulty line are set to 0, and the directed incidence matrix A^* under the typhoon disaster is constructed.
STEP3	Input the initial starting point V_s , and add the starting point to the dyeing set Q;
STEP4	Start the search from the initial starting point V_s , and select all nodes adjacent to a until the end point V_d . A search is completed, and the search result is recorded as a partition Z_1 ;
STEP5	Select other nodes except the first and last nodes of Z_1 set to search again from A^* , and record the searched path as partition Z_2 ;
STEP6	According to this search method until all nodes are traversed, the system is divided into several zones $\boldsymbol{Z} = \{Z_1, Z_2, ..., Z_N\}$, where N is the number of zones;
STEP7	Output the partition result $\boldsymbol{Z}$.

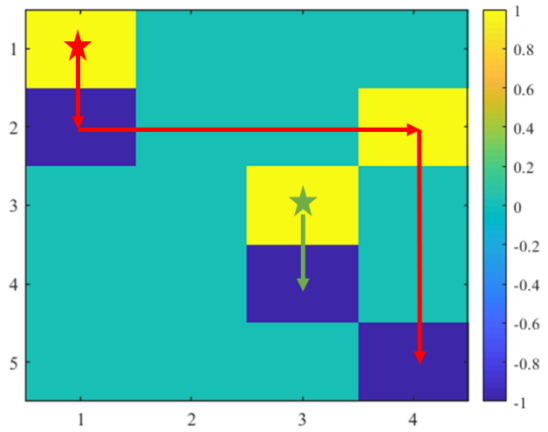

FIGURE 4. Schematic diagram of the search based on BFS of *A**.

Since the distribution grid lines are impacted by typhoons and may be disconnected, the original distribution grid is divided into several islanded microgrids, which can reduce or even avoid load shedding if these islanded microgrids contain distributed power sources (wind, PV) or energy storage devices, etc. If these islanded microgrids do not contain distributed power sources that can support the load, load shedding may occur with a high probability. Therefore, it is necessary to calculate the load shedding in each islanded

microgrid after partitioning to quantitatively study the load shedding of the system and perform resilience assessment.

B. DISTRIBUTION GRID OPTIMIZATION MODEL CONSIDERING ENERGY STORAGE

After determining the partitions, we calculate the optimal load shedding in each islanded microgrid, and the target of this optimization model is to minimize load shedding in each islanded microgrid. The time considered is the duration of the outage due to typhoon duration T. Equation (18) represents the objective function, where the load shedding in island microgrid.

Objective function:

$$Min. \sum_{t=1}^{T} \sum_{i \in \Omega_B} LC_i(t) \tag{18}$$

Constraints:

$$-P_{w,i}(t) - P_{p,i}(t) + P^c_{e,i}(t) - P^d_{e,i}(t) + \sum_{j \in \Omega_B} G_{ij} \Delta V_j - \sum_{j \in \Omega_B} B'_{ij} \theta_j - LC_{\alpha,i}(t) = -P_{D,i}(t) \tag{19}$$

$$-Q_{p,i}(t) - Q_{e,i}(t) - \sum_{j \in \Omega_B} B''_{ij} \Delta V_j - \sum_{j \in \Omega_B} G'_{ij} \theta_j - LC_{r,i}(t) = -Q_{D,i}(t) \tag{20}$$

$$P_{ij}(t) = (\Delta V_i - \Delta V_j) G_{ij} - (\theta_i - \theta_j) B_{ij} \tag{21}$$

$$Q_{ij}(t) = -(\Delta V_i - \Delta V_j) B_{ij} - (\theta_i - \theta_j) G_{ij} \tag{22}$$

$$\underline{P_{ij}(t)} \le P_{ij}(t) \le \overline{P_{ij}(t)} \tag{23}$$

$$\underline{Q_{ij}(t)} \le Q_{ij}(t) \le \overline{Q_{ij}(t)} \tag{24}$$

$$\underline{V_i(t)} \le V_i(t) \le \overline{V_i(t)} \tag{25}$$

$$\underline{\theta_i(t)} \le \theta_i(t) \le \overline{\theta_i(t)} \tag{26}$$

$$SOC_{e,i}(t) = SOC_{e,i}(t-1) + \eta^c_{e,i} \times P^c_{e,i}(t) - \frac{P^d_{e,i}(t)}{\eta^d_{e,i}} \tag{27}$$

$$\underline{SOC_{e,i}(t)} \le SOC_{e,i}(t) \le \overline{SOC_{e,i}(t)} \tag{28}$$

$$\underline{P_{w,i}} \le P_{w,i}(t) \le \overline{P_{w,i}} \tag{29}$$

$$\underline{Q_{w,i}} \le Q_{w,i}(t) \le \overline{Q_{w,i}} \tag{30}$$

$$\underline{P_{p,i}} \le P_{p,i}(t) \le \overline{P_{p,i}} \tag{31}$$

$$\underline{Q_{e,i}} \le Q_{e,i}(t) \le \overline{Q_{e,i}} \tag{32}$$

where, $LC_i(t)$ is the amount of load shedding at node i at moment t; $P_{w,i}(t)$ and $Q_{w,i}(t)$ are the active power and reactive power of wind power at node i at moment t, respectively;$P_{p,i}(t)$ is the active power output of PV at node i at moment t; $P^c_{e,i}(t)$ and $P^d_{e,i}(t)$ are the charge and discharge power of energy storage devices at node i at moment t; $Q_{e,i}(t)$ is the reactive power of energy storage devices at node i at moment t. $SOC_{e,i}(t)$ is the nuclear power state of energy storage devices at node i at moment t.

The power flow equality constraints for active power balance for the islanded microgrid operations is given in (19). Similarly, (20) represents the reactive power balance for the islanded microgrid operations at corresponding nodes. Equation (21) is the active power capacity constraint of distribution grid line. Equation (22) represents the reactive power capacity constraint of distribution grid line. Inequality constraints (23) and (24) are the constraints of the active power and reactive power of distribution grid lines from node i to node j. Inequality constraints (25) and (26) are the constraints of voltage and phase angle at node i at moment t. The state of charge (SOC) equation constraint is (27), where $\eta^c_{e,i}$ and $\eta^d_{e,i}$ are the charging and discharging efficiencies of energy storage device, respectively. Inequality constraints (28) is a security constraint of energy storage devices. Inequality constraints (29) and (31) are the constraints of active power of wind farms and photovoltaic power stations. Inequality constraints (30) and (32) are the constraints of reactive power of wind farms and photovoltaic power stations.

C. RESILIENCE ASSESSMENT MODEL

The quantitative assessment index of resilience is an important index for assessing the ability of the distribution system to resist typhoon disasters. The resilience curve of the system in response to extreme disasters is shown in Figure 5. Under normal operation, the performance of the system can be expressed by Q_0, and under the impact of a typhoon, the operating performance of the system will be affected to a certain extent, at which time the operating performance curve of the system is described by $Q(t)$. At this time the area of the shaded part enclosed by the two curves is the size of the resilience of the system in response to typhoon disasters.

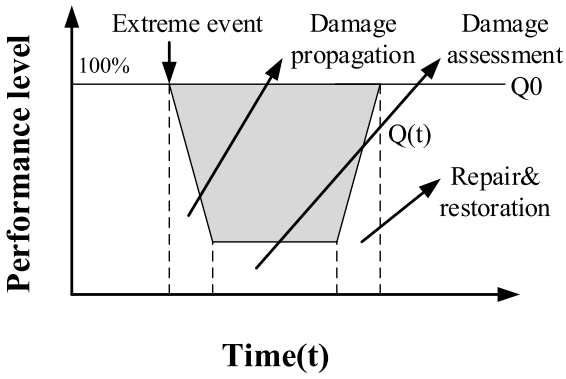

FIGURE 5. System resilience curve.

It is worth noting that the above indexes can only evaluate the resilience of the distribution system under certain disturbances. However, since the distribution system may face typhoons of different intensities, resilience under various potential typhoon hazards needs to be considered in the planning stage. In this study, we modified the resilience index to comprehensively reflect the degradation of the expected system performance under different typhoon scenarios. Typhoons are low probability and high impact events, so the probability of the event is not ignored. Therefore, the

product of the probability of typhoon occurrence and the amount of load shedding of the system during the typhoon are jointly defined as the resilience index of the system, and the index is modified as follows.

$$R = E[Q_0 - Q_1] = \sum_{w \in W} P_w (Q_0 - Q_1)_w = \sum_{w \in W} P_w Q_w \quad (33)$$

V. CASE STUDY

To verify the effectiveness of the distribution grid resilience assessment framework, the modified the IEEE 33-bus test system [21] used in this paper. The wiring diagram is shown in Figure 6. The simulation time interval is set to 1 hour and the total duration of the typhoon scenario is 24 hours. The example test in this paper was performed in MATLAB R2019b, and the hardware platform was configured as a 2.8 GHz quad-core CPU and a computer with 16 GB memory. The Distribution grid optimization model considering energy storage under typhoon disasters is the linear model. Meanwhile, the problem is solved via software packages in this paper, YALMIP and CPLEX.

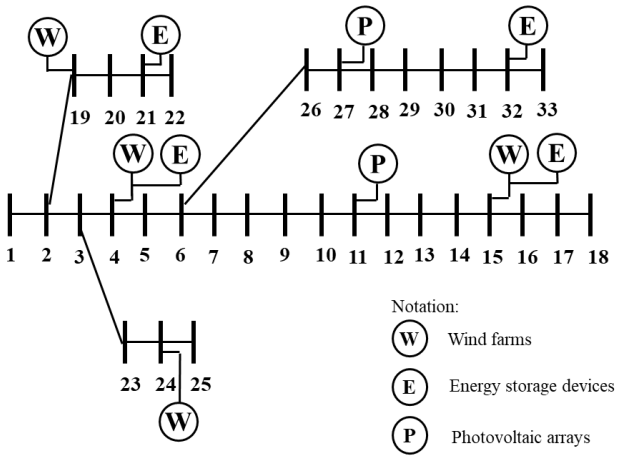

FIGURE 6. Wiring diagram of IEEE 33-bus test system.

Among them, some wind farms, PV and energy storage devices access points in IEEE 33-bus test system are shown in Table 3, which has 33 load nodes and 32 branches. The network system has a rated voltage of 12.66 kV and a total load of 3715 kW + j2300 kvar, with a minimum node voltage of 0.9169 p.u. The ESD charge and discharge efficiency is 0.95, respectively, and the rated discharge time is 6 h. The initial SOC of the ESD is assumed to be 80% of the rated capacity. The reactive power limits for WF, PV and ESD are assumed to be 70% of the rated capacity and the operating costs associated with PV and ESD are ignored.

The distribution of each key parameter of the typhoon are plotted according to the probability density function expressions of the four key parameters of the typhoon, the probability density function images of the location of the typhoon landing, the pressure difference at the center of the typhoon, the direction of the typhoon motion, and the typhoon movement speed.

TABLE 3. Distributed power supply wiring information.

Name	Node	Capacity /MW
WF	4	0.3
	15	0.2
	19	0.3
	24	0.25
PV	11	0.15
	27	0.075
ESD	4	0.4
	15	0.15
	21	0.075
	32	0.05

TABLE 4. Probability of occurrence of four key parameters of typhoons.

Pressure (hpa)	Probability	Wind speed (km/h)	Probability
58.00	0.0021	30.00	0.0171
54.08	0.0118	34.54	0.0069
61.25	0.0018	27.48	0.0423
Typhoon angle (rad)	Probability	Landing Points (E/N)	Probability
273.00	0.0004	(122,28)	0.3060
292.19	0.0002	(122.4,27.3)	0.3060
201.65	0.0007	(121.7,27.1)	0.3060

The four parameters are then randomly sampled separately to form an sample, where the probability distributions of the four key parameters of the typhoon are listed in Table 4.

Next, this IEEE 33-bus test system is placed in a real map, and Zhejiang Province is selected here as an example. According to Table 4, the free combination of the four key parameters of typhoon can form 81 sets of typical typhoon scenarios, which corresponds to an occurrence probability. Taking the first group of the four typhoon parameters as an example, the central pressure difference forming the typhoon is 58.00 hPa, the typhoon wind speed is 30 km/h, the typhoon center angle is 273.00°, and the location of typhoon landing is (122E, 28N). The trajectory of a typhoon is shown in Figure 8.

Based on the typhoon model in Section II, the wind speeds experienced by the 32 distribution lines can be calculated as shown in Figure 9.

According to the vulnerability model of the distribution grid lines in Section III, the cumulative failure probability density functions of 32 distribution lines during the passage of the typhoon are calculated, as shown in Figure 10.

Subsequently, a component-level assessment of the system was performed to identify weak lines that are more vulnerable to the typhoon. It can be found that in the calculation process of system resilience assessment, the cumulative failure probability and failure scenarios of each distribution lines can be obtained. Next, we construct a connection matrix diagram according to the wiring of the IEEE 33 system, as shown in Figure 11.

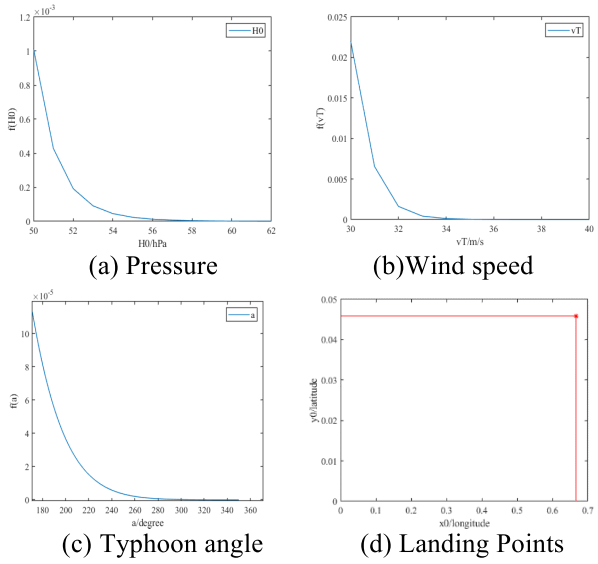

(a) Pressure (b)Wind speed (c) Typhoon angle (d) Landing Points

FIGURE 7. Probability density curve of a typhoon parameters.

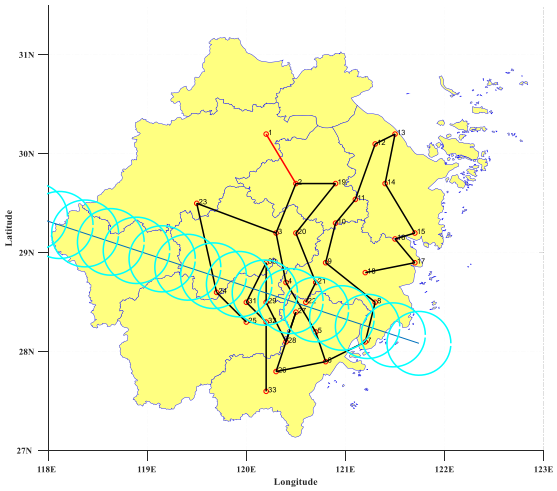

FIGURE 8. Wiring diagram in actual geographical location.

The breadth-first search algorithm is used to search the distribution network system under the typhoon scenarios, and the zoning diagram after the disaster is determined, as shown in Figure 12.

According to the results in Figure 12, in this scenarios, the IEEE 33-bus test system is divided into three subsystems under the impact of the typhoon, as shown in Figure 13.

Then the resilience indexes for the three partitions are calculated separately with and without energy storage devices, respectively, according to the resilience assessment. The results are shown in Figure 14.

As shown in Figure 14, the resilience index provides insight into the various parameters that affect resilience performance. In addition, it allows system planners to perform predictive resilience assessments and consider system enhancement strategies based on value and cost effectiveness

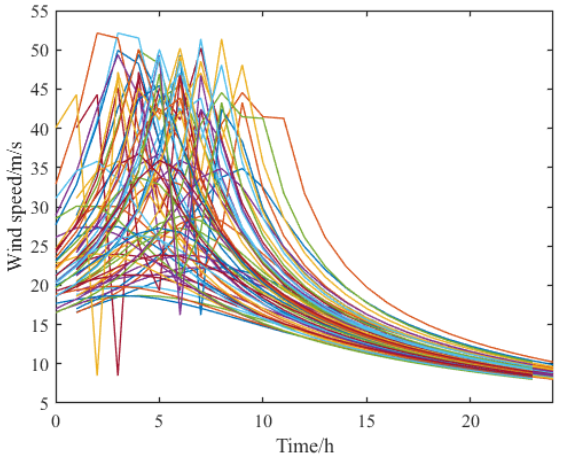

FIGURE 9. The wind speed of 32 distribution grid lines.

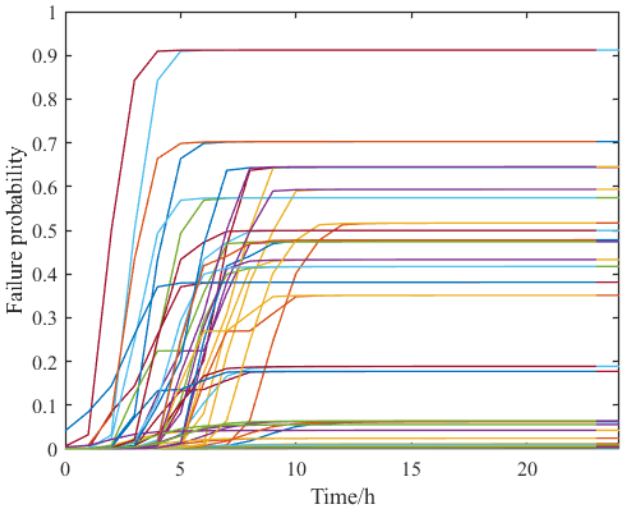

FIGURE 10. Failure probability of 32 distribution grid lines.

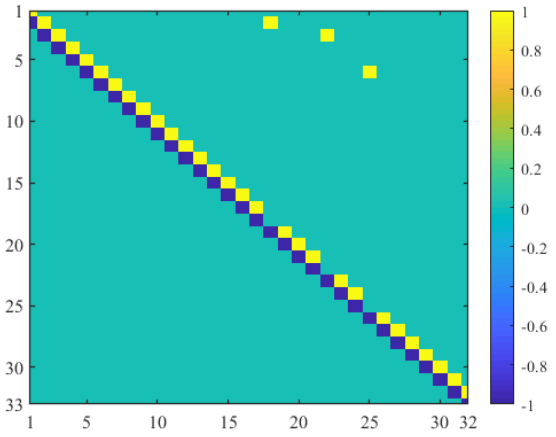

FIGURE 11. Connection matrix diagram of IEEE 33-bus test system.

aspects, and the presence of energy storage units plays an important role in the improvement of grid resilience metrics.

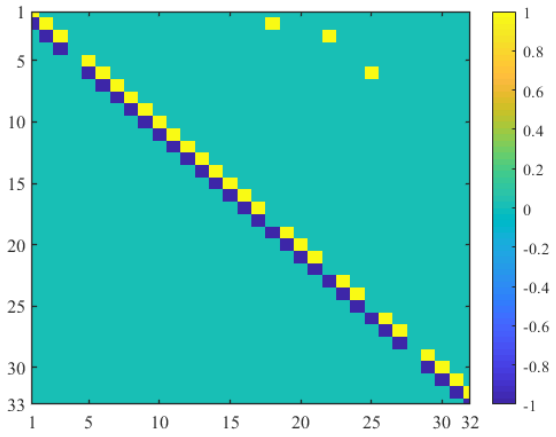

FIGURE 12. The connection matrix diagram of the IEEE 33-bus test system after the typhoon.

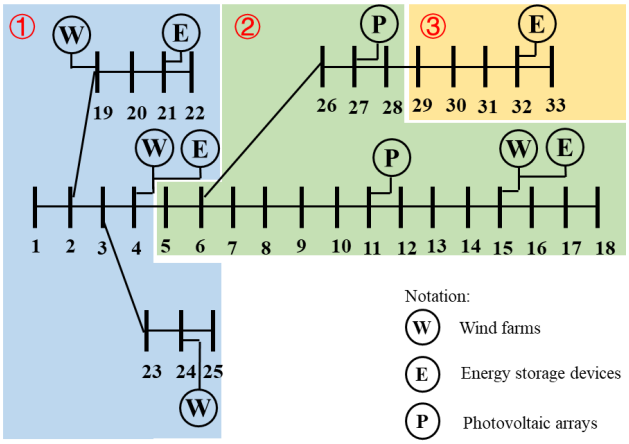

FIGURE 13. Map of island division.

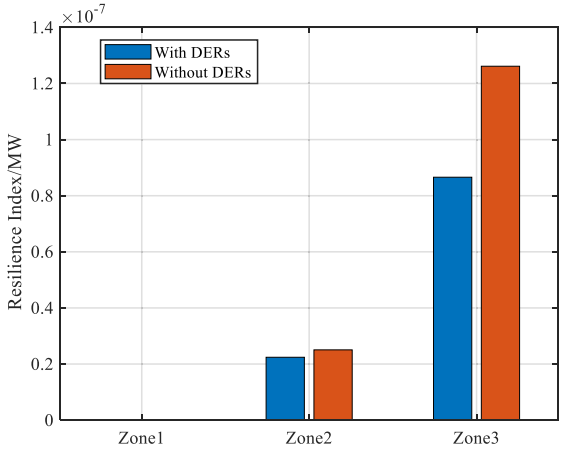

FIGURE 14. Resilience indexes of each islanded microgrid.

VI. CONCLUSION

In this paper, a resilience assessment framework for distribution systems under typhoon disasters is proposed. First, a probabilistic typhoon model is proposed that characterizes the uncertainty of typhoons through the probability distribution of core parameters. This allows us to generate a range of typhoon scenarios and corresponding occurrence probabilities. Second, spatial and temporal vulnerability models for distribution grid lines are developed considering the movement and decay of typhoons. These models quantify the relationship between the failure probability of each distribution grid line and the wind speed in terms of time and space scales. Finally, considering the impact of typhoons on distribution grid lines, a BFS algorithm is performed to establish partitions to calculate the optimal amount of load shedding for each partition, and a new resilience index is developed to quantify the resilience of the distribution system from the system and building block perspectives.

As shown in Figure 14, the resilience index of scenarios with DERs in Zone 2 and Zone 3 are 2.24×10^{-8} MW and 8.66×10^{-8} MW. Nevertheless, the resilience index of scenarios without DERs in Zone 2 and Zone 3 are 2.51×10^{-8} MW and 1.26×10^{-7} MW. If the distribution grid is equipped with energy storage devices, the resilience of the system will be improved at each islanded microgrid under typhoon disaster. The numerical results verify the accuracy and validity of the framework. The results can also provide insight into potential resilience enhancement measures for similar or unforeseen typhoon hazards in the future. This method can effectively and economically expand and upgrade the planned distribution system. In the future, we will expand the study to include prevention and enhancement of restoration measures. In addition, the impact of interactions between adjacent lines is not considered in this paper, and we will establish the interactions between lines to address this issue in the future.

REFERENCES

[1] Z. Bie, Y. Lin, G. Li, and F. Li, "Battling the extreme: A study on the power system resilience," *Proc. IEEE*, vol. 105, no. 7, pp. 1253–1266, Jul. 2017.

[2] G. Huang, J. Wang, C. Chen, J. Qi, and C. Guo, "Integration of preventive and emergency responses for power grid resilience enhancement," *IEEE Trans. Power Syst.*, vol. 32, no. 6, pp. 4451–4463, Nov. 2017.

[3] L. R. Russell and G. I. Schueller, "Probabilistic models for Texas Guif coast hurricane occurrences," *J. Petroleum Technol.*, vol. 26, no. 3, pp. 279–288, 1974.

[4] M. E. Batts, "Hurricane wind speeds in the United States," *J. Struct. Division*, vol. 106, no. 10, pp. 2001–2016, 1980.

[5] P. N. Georgiou, "Design wind speeds in tropical cyclone-prone regions," Ph.D. dissertation, Western Ontario Univ., London, ON, Canada, 1985.

[6] S. Lin, W. Fang, X. Wu, Y. Chen, and Z. Huang, "A spark-based high performance computational approach for simulating typhoon wind fields," *IEEE Access*, vol. 6, pp. 39072–39085, 2018.

[7] H. Li, S. Gao, G. Liu, D. Guo, C. Grecos, and P. Ren, "Visual prediction of typhoon clouds with hierarchical generative adversarial networks," *IEEE Geosci. Remote Sens. Lett.*, vol. 17, no. 9, pp. 1478–1482, Sep. 2020.

[8] S. Ma, L. Su, Z. Wang, F. Qiu, and G. Guo, "Resilience enhancement of distribution grids against extreme weather events," *IEEE Trans. Power Syst.*, vol. 33, no. 5, pp. 4842–4853, Sep. 2018.

[9] S. Ma, B. Chen, and Z. Wang, "Resilience enhancement strategy for distribution systems under extreme weather events," *IEEE Trans. Smart Grid*, vol. 9, no. 2, pp. 1442–1451, Mar. 2018.

[10] W. Yuan, J. Wang, F. Qiu, C. Chen, C. Kang, and B. Zeng, "Robust optimization-based resilient distribution network planning against natural disasters," *IEEE Trans. Smart Grid*, vol. 7, no. 6, pp. 2817–2826, Nov. 2016.

[11] M. Panteli and P. Mancarella, "Operational resilience assessment of power systems under extreme weather and loading conditions," in *Proc. IEEE Power Energy Soc. Gen. Meeting*, Jul. 2015, pp. 1–5.
[12] M. Panteli, D. N. Trakas, P. Mancarella, and N. D. Hatziargyriou, "Boosting the power grid resilience to extreme weather events using defensive islanding," *IEEE Trans. Smart Grid*, vol. 7, no. 6, pp. 2913–2922, Nov. 2016.
[13] T. Ding, M. Qu, Z. Wang, B. Chen, C. Chen, and M. Shahidehpour, "Power system resilience enhancement in typhoons using a three-stage day-ahead unit commitment," *IEEE Trans. Smart Grid*, vol. 12, no. 3, pp. 2153–2164, May 2021.
[14] M. Ouyang and Z. Wang, "Resilience assessment of interdependent infrastructure systems: With a focus on joint restoration modeling and analysis," *Rel. Eng. Syst. Saf.*, vol. 141, pp. 74–82, Sep. 2015.
[15] S. Chanda, A. K. Srivastava, M. U. Mohanpurkar, and R. Hovsapian, "Quantifying power distribution system resiliency using code based metric," in *Proc. IEEE Int. Conf. Power Electron., Drives Energy Syst. (PEDES)*, Dec. 2016, pp. 1–6.
[16] J. Najafi, A. Peiravi, and J. M. Guerrero, "Power distribution system improvement planning under hurricanes based on a new resilience index," *Sustain. Cities Soc.*, vol. 39, pp. 592–604, May 2018.
[17] Y. Yang, W. Tang, Y. Liu, Y. Xin, and Q. Wu, "Quantitative resilience assessment for power transmission systems under typhoon weather," *IEEE Access*, vol. 6, pp. 40747–40756, 2018.
[18] P. Eder-Neuhauser, T. Zseby, and J. Fabini, "Resilience and security: A qualitative survey of urban smart grid architectures," *IEEE Access*, vol. 4, pp. 839–848, 2016.
[19] P. Gautam, P. Piya, and R. Karki, "Resilience assessment of distribution systems integrated with distributed energy resources," *IEEE Trans. Sustain. Energy*, vol. 12, no. 1, pp. 338–348, Jan. 2021.
[20] Y. Shi, Q. Zhang, S. Wang, K. Yang, Y. Yang, and Y. Ma, "Impact of typhoon on evaporation duct in the northwest Pacific Ocean," *IEEE Access*, vol. 7, pp. 109111–109119, 2019.
[21] M. E. Baran and F. F. Wu, "Network reconfiguration in distribution systems for loss reduction and load balancing," *IEEE Trans. Power Del.*, vol. 4, no. 2, pp. 1401–1407, Apr. 1989.

YUANTAO WANG is currently a Senior Engineer at Hangzhou Power Supply Company. His current research interests include power system operation and optimization.

TIANEN HUANG received the bachelor's and Ph.D. degrees in electrical engineering from Tsinghua University, China, in 2014 and 2019, respectively. He is currently a Senior Engineer at Hangzhou Power Supply Company. His research interests include security knowledge discovery, big data analysis, and application of machine-learning methods in power systems.

XIANG LI is currently a Senior Engineer at Hangzhou Power Supply Company. His interests include power system operation, control and information theory applied to power systems, power system reliability, and parallel computing techniques in power systems.

JIAN TANG is currently a Senior Engineer at Hangzhou Power Supply Company. His research interests include areas of power system reliability, planning, and analysis.

ZHENJIE WU is currently a Senior Engineer at Hangzhou Power Supply Company. His current research interests include power system operation and optimization.

YAJUN MO is currently a Senior Engineer at Hangzhou Power Supply Company. His research interests include power system operation and optimization and power system reliability assessment.

LIN XUE received the B.S. degree in electrical engineering from Qinghai University, Qinghai, China, in 2020. He is currently pursuing the master's degree with the School of Electrical Engineering, Chongqing University. His current research interest includes dynamic reactive power reserve assessment of wind farms.

YIXI ZHOU is currently a Senior Engineer at Hangzhou Power Supply Company. His research interests include multi-energy system dis-patching automation and smart grid control theory.

TAO NIU (Member, IEEE) received the B.S. and Ph.D. degrees from the Department of Electrical Engineering, Tsinghua University, Beijing, China, in 2014 and 2019, respectively. He is currently an Assistant Professor with Chongqing University, Chongqing, China. His research interests include power system operation and optimization, power system reliability assessment, voltage security region, automatic reactive power voltage control, renewable generation integration, and reactive power analysis of hybrid AC/DC systems.

SICONG SUN is currently a Senior Engineer at Hangzhou Power Supply Company. His current research interests include power system operation and optimization.